Reports

Uplifted Marine Terraces Along the Alpine Fault, New Zealand

William B. Bull and Alan F. Cooper

Three types of evidence indicate that marine terraces are widespread in the Southern Alps of New Zealand. (i) Remnants of shore platforms occur as distinct levels of notched ridge crests and flat summits; degraded sea cliffs are common. (ii) Scattered quartz beach pebbles occur on 16 of 18 levels of exhumed shore platforms in the Fox–Franz Josef type area to altitudes as high as 1700 meters. (iii) Altitudinal spacings of New Zealand terrace flights allow correlation with 18 dated global marine terraces at New Guinea, which were formed during glacio-eustatic highstands of sea level within the last 336 × 10^3 years. Inferred uplift rates at Fox–Franz Josef increased from 3.2 to 7.8 meters per 10^3 years since about 135 × 10^3 to 140 × 10^3 years ago, presumably because of increased convergence between the Pacific and Australian plates.

Marine terraces formed during global eustatic sea-level highstands are time lines in rising coastal landscapes. Undated and dated terraces may be correlated because unique altitudinal spacings are associated with each uniform uplift rate. Our model for marine-terrace spacing is conceptually the same as that used for the spacing of sea-floor magnetic stripes. Nonuniform time spans between global magnetic polarity reversals create a variable pattern of magnetic anomalies, even though crustal spreading rates are uniform. Each spreading rate has a unique spacing of magnetic stripes (*1*). Nonuniform intervals between times of marine-terrace formation and nonuniform altitudes of formation (*2*) create a variable altitudinal spacing for flights of marine terraces, even where uplift rates are uniform. Each uplift rate has a unique altitudinal spacing of terraces. The models for spacings of global ocean-floor magnetic anomalies and global marine-terrace altitudes can be used to infer ages where radiometric age determinations are not available; both require careful dating in type localities. The Th/U ages of New Guinea corals provide dates for most major terraces formed during the last 336 × 10^3 years (*3*); other dates come from sedimentation and reef growth rates. This report summarizes the evidence for ancient shorelines in the Southern Alps of New Zealand and for uniform uplift during the last 135 × 10^3 to 140 × 10^3 years and describes inferred uplift rates.

The tectonic setting of the Southern Alps is the result of juxtaposition of continental crusts of the Australian and Pacific plates along the Alpine fault (Fig. 1). Relative plate motion near the middle of the Alps is about 46 m per 10^3 years; it can be resolved into dextral motion parallel to the Alpine fault of 40 m per 10^3 years and shortening perpendicular to the fault of 22 m per 10^3 years (*4*). Crustal shortening is achieved by uplift and by development of a root zone of thickened Pacific plate crust in the north and underthrust Australian plate crust in the south (*4*). Schist and graywacke are being vigorously eroded by rivers and glaciers. Adams (*5*) proposed that the Alps are being worn down as fast as the postulated 20 m per 10^3 years at which they are being uplifted. Other studies suggest lesser rates of uplift [5 m per 10^3 years (*6*)] and denudation [11 to 13 m per 10^3 years (*7*)].

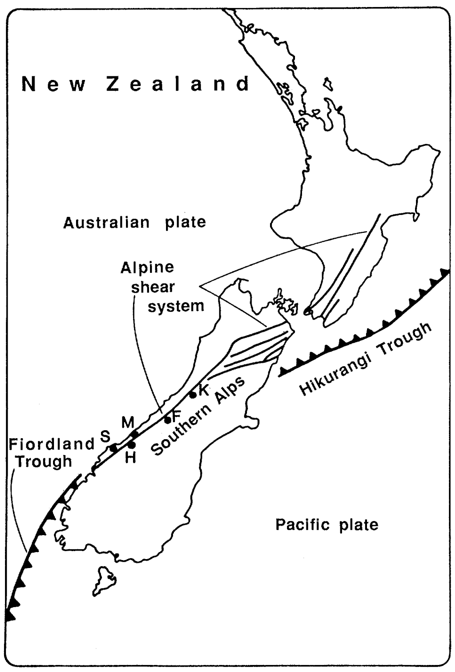

Fig. 1. Tectonic setting of New Zealand and locations of study sites at Kaniere (K), Fox–Franz Josef (F), Haast River (H), Moeraki River (M), and Stafford Range (S).

Recognition of two high (960 and 1430 m) remnants of marine terraces east of the Alpine fault (*6*) poses questions as to whether more terrace remnants are present, and whether they occur elsewhere in the Alps. We believe that flights of late Quaternary marine terraces are present both east and west of the Alpine fault and that they can be correlated with the dated New Guinea terraces to provide insight regarding styles and rates of uplift along the plate boundary.

Spur and main divide ridges are prominently notched to altitudes of more than 3000 m. Initially, most notches were sea cliffs and associated shore platforms that presently are formed in the intertidal range (*8*). Below altitudes of 1700 m in three study areas (Fig. 1), the landforms have survived erosion sufficiently well to be recognized as exhumed shore platforms and degraded sea cliffs cut in fairly homogeneous schist.

The morphologies of the marine-terrace remnants vary with altitude and age. Locally, continuous strandlines can be traced for 1 to 3 km. High remnants consist of broad summits and flat ridge crests as much as 1 km long (Fig. 2). Notched spur ridges dominate at intermediate altitudes (400 to 1400 m), each notch consisting of a sloping shore-platform remnant and its associated adjacent sea-cliff remnant. At altitudes of only a few hundred meters the terrace remnants occur as benches notched into mountain-front escarpments. Low bedrock benches are mantled with colluvium and, along some valleys, merge with remnants of fluvial straths that were graded to the same former sea-level highstands.

Beach pebbles occur on the notched spurs and flat summits. Angular quartz fragments are weathered from schist. Widely scattered but exceptionally well-rounded quartz pebbles and cobbles contrast markedly with the angular quartz pebbles. A fluvial origin is improbable for rounded pebbles on flat summits. Scanning electron microscopy of rounded quartz grains from terrace remnants reveals surface textures similar to those of modern beach pebbles (*6*). The beach pebbles were probably stored in bedrock fractures and topographic lows and have been exhumed by erosion of sea-cliff colluvium.

Additional evidence for the presence of marine terraces is the correlation of the ten youngest terraces with dated New Guinea terraces. The conceptual model, methodolo-

W. B. Bull, Geosciences Department, University of Arizona, Tucson, AZ 85721.
A. F. Cooper, Geology Department, University of Otago, Post Office Box 56, Dunedin, New Zealand.

Table 1. Altitudes of notched ridge crests along two transects on Cole Spur near Franz Josef. From map NZMS 1 Waiho S71. Only altitudes in parentheses are used in Table 2 and Fig. 2.

North of Stony Creek		South of Stony Creek	
Altitude (feet) (*10*)	Grid reference map location	Altitude (feet) (*10*)	Grid reference map location
650*	857758	650 198 m*	855754
		950 (290 m)	858752
1050	866764	1050 (320 m)	853746
1450	864754	1450 (442 m)	854744
1650	865755	1650 (503 m)	861747
1850–1950	866755	1850 (564 m)	862746
2150	867755	2150 (655 m)	856740
		2350–2450 (747 m)	860740
2350	869755		865744
2550 (777 m)	873751		
2950	875749	2950 (899 m)	870743
3250–3350	878748	3250 (991 m)	874740
3750	883746	3750 (1143 m)	880738
4250	886742	4250 (1296 m)	884738

*Mountain-piedmont junction may coincide with base of sea cliff formed at 30×10^3 years, but the 198-m altitude is not used in the Table 2–Fig. 2 analysis.

gy, pitfalls, and cross-checks of global-marine terrace correlation by altitudinal spacing analysis are discussed in detail by Bull (*2*).

Glacio-eustatic fluctuations in late Pleistocene sea level control the ages and partly determine the altitudes of marine terraces. Studies in the Atlantic and Pacific oceans show that marine terraces formed at 6 m above to 46 m below present sea level during the last 336×10^3 years. Global synchroneity of the 120×10^3 year terrace and several others is demonstrated by uranium-series disequilibrium dating of coral from New Guinea, New Hebrides, Barbados, Haiti, the Mediterranean Sea, Hawaii, Japan, and California (*3, 9*). We assume that major sea-level changes occurred synchronously at New Guinea and New Zealand.

Attempts to correlate New Zealand with New Guinea marine terraces are illustrated in Figs. 2 and 3; data are listed in Tables 1, 2, and 3. We first consider a sampling of altitudes of ancient shorelines from a pair of ridge crests along 3 km of mountain front, and then consider variations of inferred uplift rates for 20- and 250-km-long study areas adjacent to the Alpine fault.

About 7 km east of Franz Josef a triangular facet rises 1600 m from the trace of the Alpine fault to Cole Spur over a distance of 4.7 km. The facet is dissected by Stony Creek, which has cut a valley 300 m deep in a 3-km^2 watershed. The ridge crests in this glacially unmodified landscape retain remnants of shore platforms at bases of degraded sea cliffs. Altitudes and locations of accordant notches are listed in Table 1 and the quality of data is discussed in (*10*). The mountain-piedmont junction is at 200 m, above which 10 of 12 notches are accordant. Each ridge crest apparently is missing one level of notched spur. The altitudes of notched spurs on the south ridge crest and the 777-m altitude on the north ridge crest are used in the following correlation attempts.

Assignment of a New Guinea age to one local terrace results in sequential age assignments for all other terraces. For correlation attempt A in Table 2, the 503-m terrace remnant is assigned an age of 30×10^3 years and has an inferred uplift of 545 m [503 m − (−42 m)]. All four correlation attempts can be fitted with regression lines (Fig. 2) that indicate consistently rapid uplift (6 to 10 m per 10^3 years), and all indicate slower uplift before 133×10^3 years ago. Only plot B passes through the graph origin, which indicates uniform uplift for the last 133×10^3 years.

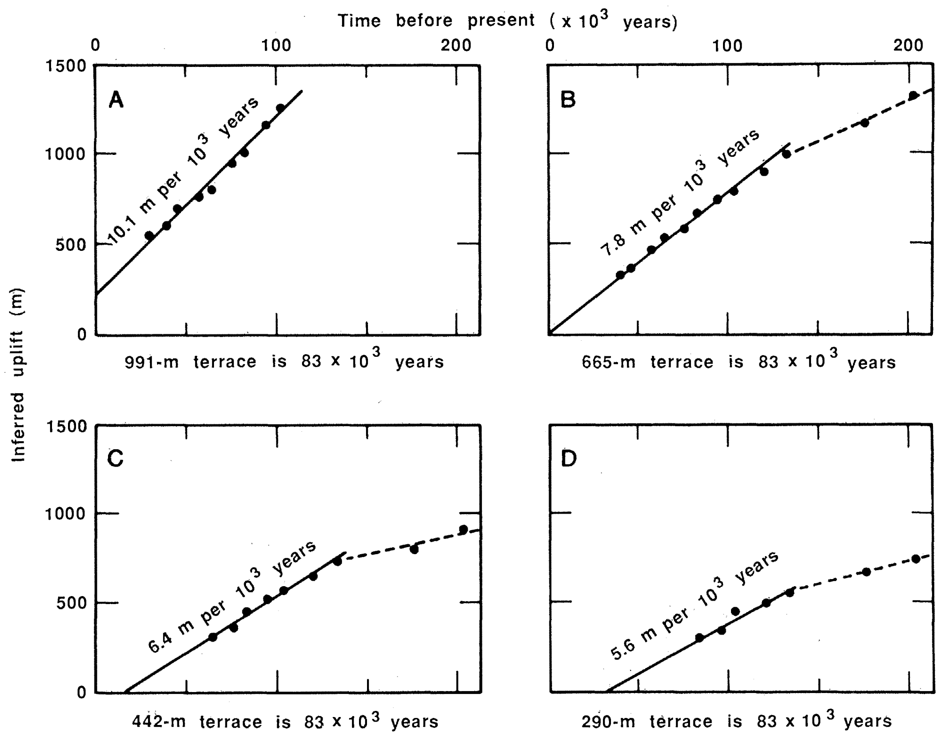

Fig. 2. Attempted correlations of a flight of marine-terrace remnants on a ridge crest north of Stony Creek near Franz Josef, with dated marine terraces in New Guinea. Labels correspond to correlations in Table 2. (A) Terrace remnant 503 m high assigned an age of 30×10^3 years. (B) Terrace 290 m high assigned an age of 40×10^3 years. (C) Terrace 290 m high assigned an age of 64×10^3 years. (D) Terrace 290 m high assigned an age of 83×10^3 years. Only (B) portrays uniform uplift; the line passes through the data points and the origin.

Which correlation is most reasonable? Plot A (Fig. 2) ignores the presence of three terrace levels on Cole Spur, and, because the regression line intersects the ordinate at 230 m, one must also assume a rapid increase in uplift rate to more than 20 m per 10^3 years at some time since 30×10^3 years ago. Plots C and D assume that many young New Guinea terrace correlatives are not present despite the apparently rapid uplift rate, and that either uniform uplift abruptly ceased at 15×10^3 and 30×10^3 years ago, respectively, or that there have been pronounced declines in uplift rates since 64×10^3 or 83×10^3 years ago. Plot B assumes that uniform uplift has continued to the present. Only correlation B accounts for all of the New Zealand and all of the New Guinea terraces. We conclude that B is the most reasonable correlation and infer that this small part of the Southern Alps has been rising uniformly at 7.8 m per 10^3 years during the last 133×10^3 years.

How large an area can be represented by the inferred uplift rate of 7.8 m per 10^3 years? Does the uplift rate change to the southeast of the Alpine fault? Was there an

lift rate 135 × 10^3 to
ago? We addressed these
›ulating altitudes of 436
ive of marine-terrace rem-
0 km by 6 km southeast of
›y making the same type of
·le Spur (Table 3).
ıata must be accurate if we
ssful correlations of global
ncluding the age determi-
Jew Guinea terraces, alti-
n, and present terrace alti-
:w Guinea and New Zea-
ınt assumption is that re-
were uniform at both the
New Zealand study areas.
on in any of these factors
:er around regression lines
ı the origin.
ɔlift rate at Fox–Franz Jo-
ı 3.1 to 7.8 m per 10^3 years
140 × 10^3 years ago. The
ıiformity of recent uplift
Spur and Fox–Franz Josef
st that large sections of the
: being uplifted at the same
n per 10^3 years) and that
not change rapidly with
:e east of the Alpine fault.
tes before 135 × 10^3 to
ago were conducive to the
:xtensive shore platforms.
regional variations in in-
ılong 250 km of the Alpine
:wo additional analyses. A
of the fault was studied.
l uplift for the Kaniere,
d Fox–Franz Josef study
3) reveal uniform inferred

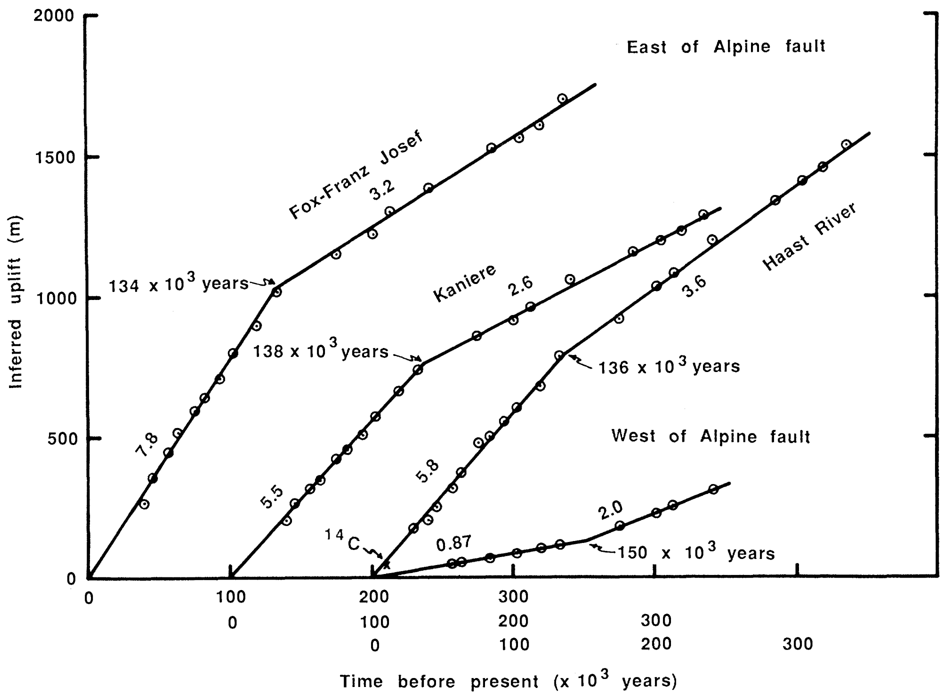

Fig. 3. Inferred uplift rate graphs for flights of marine-terrace remnants along the Alpine fault in the Fig. 1 study areas. Carbon-14 date is from (*6*). All rates are in meters per 10^3 years, and are labeled on the associated graph. Each curve is shifted for clarity, with shifted scales starting at the time-axis intercepts.

uplift rates during the last 135 × 10^3 to 140 × 10^3 years of 5.5, 5.9, and 7.8 m per 10^3 years, respectively.

The pattern of uplift rates for the 200 × 10^3 years before about 140 × 10^3 years is different in all three study areas east of the Alpine fault. Inferred uplift rates were uniform but much less, being only 2.6 m per 10^3 years at Kaniere, 3.2 m per 10^3 years at Fox–Franz Josef, and 3.6 m per 10^3 years at Haast River. There appears to be a 40% increase in uplift rates 340 × 10^3 to 140 × 10^3 years ago toward the southwest. This may partly explain an anomaly: al-

l correlations of the Cole Spur marine-terrace remnants with the dated sequence of ıces at New Guinea (*3*). Values vary in precision (*10*). Abbreviations: *M*, mean *U*, inferred uplift in meters.

.e .1	New Zealand terraces							
	M	*U*	*M*	*U*	*M*	*U*	*M*	*U*
	A							
	503	545						
			B					
	564	601	290	327				
	655	692	320	357				
	732	761	442	471				
					C			
	777	803	503	529	290	316		
	899	945	564	610	320	366		
							D	
	991	1004	655	668	442	455	290	303
	1143	1163	732	752	503	523	320	340
	1246	1256	777	787	564	574	442	452
			899	893	655	649	503	497
			991	986	732	727	564	559
			1143	1164	777	798	655	676
			1296	1313	899	916	732	749

Table 3. Best correlation of the inferred uplift of the Fox–Franz Josef marine-terrace sequence with the dated New Guinea terraces. Ages and altitudes of formation at the left are from Chappell (*3*); data for the Fox–Franz Josef terraces are on the right side. The rows of the two sides are aligned to show the most logical correlation, which is the 7.8 m per 10^3 years plot of Fig. 3. Values vary in precision (*10*).

New Guinea terraces		New Zealand terraces	
Age (×10^3 years)	Altitude formed (m)	Altitude (m)	Inferred uplift (m)
40	−37	229	266
46	−37	320	357
57	−29	412	441
64	−26	488	514
76	−46	549	595
83	−13	625	638
94	−20	686	706
103	−10	793	803
120	+6	899	893
133	+5	1021	1016
176	−21	1128	1149
202	−17	1204	1221
214	−3	1296	1299
242	−28	1357	1385
286	−46	1479	1525
305	−27	1540	1567
320	+4	1616	1612
336	+4	1707	1703

though the highest peaks of the Southern Alps occur southeast of Franz Josef, where after 140×10^3 years ago uplift is inferred to be maximum, the area of highest metamorphic grade of schist and hence expected maximum total uplift occurs 25 to 40 km northeast of the Haast River.

The close altitudinal spacing of marine terraces along the coast west of the Alpine fault between the Stafford Range and the Moeraki River suggests relatively low uplift rates, so we surveyed altitudes of uplifted shore platforms in conjunction with topographic map analyses. Attempts to correlate six marine terraces in the coastal mountains with New Guinea terraces yielded only one reasonable solution (Fig. 3). Uniform inferred uplift of 2.0 m per 10^3 years between 242×10^3 and 176×10^3 years ago decreased to uniform uplift of 0.87 m per 10^3 years since roughly 150×10^3 years ago.

Correlations of remnants of marine terraces along the northwestern flank of the Southern Alps at three widely spaced sites with the dated sequence of global marine terraces at New Guinea is a useful basis for inferring terrace ages and uplift rates. At least 250 km of the Southern Alps is being elevated at an inferred rate of 5 to 8 m per 10^3 years during the last 135×10^3 to 140×10^3 years. Reset K/Ar radiometric clocks in heated and uplifted schist, and surficial temperature gradients, imply uplift rates of less than 10 m per 10^3 years (*11*); these cross-checks agree with the uplift rates inferred from the marine-terrace analyses. An apparent doubling of uplift rate occurred between 135×10^3 years and 140×10^3 years ago at three widely separated sites east of the Alpine fault. Presumably, it is associated with long-term increasing convergence between the Australian and Pacific plates. Opposite and roughly synchronous changes in inferred uplift rates east and west of the Alpine fault near the Haast River also contribute to the picture of internal consistency that supports the correlations and uniform uplift-rate assumption.

REFERENCES AND NOTES

1. F. J. Vine and D. H. Matthews, *Nature (London)* **199**, 947 (1963); J. Heirtzler *et al.*, *J. Geophys. Res.* 73, 2119 (1968).
2. W. B. Bull, in *Proceedings of the 15th Annual Binghamton Geomorphology Symposium*, M. Morisawa and J. T. Hack, Eds. (Allen and Unwin, Hemel Hempstead, United Kingdom, 1985), p. 129–152.
3. A. L. Bloom, W. S. Broecker, J. M. A. Chappell, R. K. Matthews, K. J. Mesolella, *Quat. Res. (N.Y.)* **4**, 185 (1974); J. M. A. Chappell, *Geol. Soc. Am. Bull.* **85**, 553 (1974); *Search* **14**, 99 (1983); written communication, 13 January 1983.
4. R. J. Walcott, *Bull. R. Soc. N.Z.* **18**, 4 (1979); J. Adams, *Geol. Soc. Am. Bull.* **91**, 1 (1980).
5. J. Adams, *Bull. R. Soc. N.Z.* **18**, 47 (1979).
6. A. F. Cooper and D. G. Bishop, *ibid.*, p. 35; G. J. van der Lingen, *ibid.*, p. 45.
7. A. G. Griffiths and M. J. McSaveny, *N.Z. J. Sci.* **26**, 293 (1983); M. R. Hawkes, thesis, University of Canterbury, Christchurch, New Zealand (1981).
8. R. M. Kirk, *N.Z. J. Geol. Geophys.* **20**, 571 (1977); W. C. Bradley and G. B. Griggs, *Geol. Soc. Am. Bull.* **87**, 433 (1976).
9. F. W. Taylor, C. Jouannic, A. L. Bloom, *J. Geol.* **93**, 419 (1985); R. K. Matthews, *Quat. Res. (N.Y.)* **3**, 147 (1973); R. E. Dodge, R.G. Fairbanks, L. K. Benninger, F. Maurrasse, *Science* **219**, 1423 (1983); P. J. Hearty, G. H. Miller, C. E. Stearns, B. J. Szabo, *Geol. Soc. Am. Bull.* **97**, 850 (1986); T. L. Ku, M. A. Kimmel, W. H . Easton, T. J. O'Neil, *Science* **183**, 959 (1974); T. Yoshikawa, Y. Ota, N. Yonekura, A. Okada, N. Iso, *Geog. Rev. Jpn.* **53**, 238 (1980); T. Yoshikawa, S. Kaizuka, Y. Ota, *The Landforms of Japan* (Univ. of Tokyo Press, Tokyo, 1981); T. L. Ku and J. P. Kern, *Geol. Soc. Am. Bull.* **85**, 1713 (1974).
10. Best age control is 133×10^3 years and younger ($\pm 3 \times 10^3$ years to 5×10^3 years), poorest is older than 214×10^3 years ($\pm 10 \times 10^3$ years to 15×10^3 years). Altitudes formed are ± 5 m, mean altitudes ± 15 m, and inferred uplift ± 20 m.
11. R. G. Allis, *Geology* **9**, 303 (1981); *International Symposium on Recent Crustal Movements Abstracts* (Royal Society of New Zealand, Wellington, 1984), p. 1.

12. We appreciate discussions with K. R. Berryman, A. L. Bloom, J. Bradshaw, J. Campbell, J. M. A. Chappell, B. Harrison, R. M. Kirk, P. L. K. Knuepfer, K. R. Lajoie, Y. Ota, R. P. Suggate, and H. W. Wellman. Supported by National Science Foundation grants EAR-815836 and EAR-8305892, U.S. Geological Survey contract 14-08-0001-21882, and the Otago University Research Grants Committee.

17 April 1986; accepted 19 August 1986

Polymorphism of Sickle Cell Hemoglobin Aggregates: Structural Basis for Limited Radial Growth

LEE MAKOWSKI AND BEATRICE MAGDOFF-FAIRCHILD

Fibers composed of molecules of deoxygenated sickle cell hemoglobin are the basic cause of pathology in sickle cell disease. The hemoglobin molecules in these fibers are arranged in double strands that twist around one another with a long axial repeat. These fibrous aggregates exhibit a pattern of polymorphism in which the ratio of their helical pitch to their radius is approximately constant. The observed ratio agrees with an estimate of its value calculated from the geometric properties of helical assemblies and the degree of distortion that a protein-protein interface can undergo. This agreement indicates that the radius of an aggregate is limited by the maximum possible stretching of double strands. The geometric properties limiting the radial extent of sickle hemoglobin fibers are fundamental to all cables of protein filaments and could contribute to the control of diameter in other biological fibers such as collagen or fibrin.

SICKLE CELL HEMOGLOBIN DIFFERS from normal hemoglobin only in that a valyl residue is substituted for a glutamate at the β6 position of both β chains of the molecule. In its unliganded state, the sickle cell hemoglobin (HbS) molecule has a lower solubility than normal hemoglobin. This results in an aggregation of the molecules into regular fibrous arrays. Much of the pathophysiology of sickle cell disease is attributed to occlusion of the capillaries in the microcirculation by fiber-containing erythrocytes. Observed polymorphic assemblies in vitro range in size from 220 Å diameter fibers (*1*) to larger macrofibers (*2, 3*), twisted crystals (*4*), and macroscopic crystals suitable for high-resolution x-ray crystallography (*5–7*). The crystals and the fibers found in erythrocytes and in solutions of deoxy-HbS have a common basic structural element, the presence of which has been confirmed by the striking similarities of their x-ray diffraction patterns (*8, 9*). This basic structural unit or protofilament is a double strand of HbS molecules, which possesses approximate twofold screw symmetry with an axial rise of 32 Å per hemoglobin molecule. The protofilament is stabilized, in part, by the interaction of one of the β6 residues in HbS with the edge of the heme pocket of an adjacent molecule (*7, 10*).

All of the aggregates of HbS molecules are side-to-side assemblies of the protofilaments. In the macroscopic crystals, the protofilaments are arranged parallel or antiparallel to one another. In the smaller aggregates, the protofilaments are slightly twisted, and coil around one another with a long helical pitch. From the side-to-side packing of protofilaments in the fibrous aggregates, it would appear possible to continue adding protofilaments to these aggregates without bound. The side-to-side packing of protofilaments is not self-limiting as it is, for instance, in the case of microtubules, where

L. Makowski, Department of Biochemistry and Molecular Biophysics, Columbia University, College of Physicians and Surgeons, 630 West 168 Street, New York, NY 10032.
B. Magdoff-Fairchild, Department of Medicine, Columbia University, College of Physicians and Surgeons, and Hematology Division, Medical Service St. Luke's–Roosevelt Hospital Center, New York, NY 10025.